Takahisa Nakamura, Alessandro Arduini, Brenna Baccaro, Masato Furuhashi, and Gökhan S. Hotamisligil

Small-Molecule Inhibitors of PKR Improve Glucose Homeostasis in Obese Diabetic Mice

SIGNAL TRANSDUCTION

Obesity and metabolic diseases appear as clusters, often featuring high risk for insulin resistance and type 2 diabetes, and constitute a major global health problem with limited treatment options. Previous studies have shown that double-stranded RNA–dependent kinase, PKR, plays an important role in the nutrient/pathogen-sensing interface, and acts as a key modulator of chronic metabolic inflammation, insulin sensitivity, and glucose homeostasis in obesity. Recently, pathological PKR activation was also demonstrated in obese humans, strengthening its prospects as a potential drug target. Here, we investigate the use of two structurally distinct small-molecule inhibitors of PKR in the treatment of insulin resistance and type 2 diabetes in cells and in a mouse model of severe obesity and insulin resistance. Inhibition of PKR reduced stress-induced Jun NH_2-terminal kinase activation and insulin receptor substrate 1 serine phosphorylation in vitro and in vivo. In addition, treatment with both PKR inhibitors reduced adipose tissue inflammation, improved insulin sensitivity, and improved glucose intolerance in mice after the establishment of obesity and insulin resistance. Our findings suggest that pharmacologically targeting PKR may be an effective therapeutic strategy for the treatment of insulin resistance and type 2 diabetes.

Diabetes 2014;63:526–534 | DOI: 10.2337/db13-1019

The link between cellular stress signals and chronic metabolic diseases, including obesity-induced insulin resistance, type 2 diabetes, fatty liver disease, and atherosclerosis, has been well-established (1–3). During the course of obesity a broad array of inflammatory and stress responses are evoked in metabolic tissues, leading to activation of several inflammatory signaling molecules including Jun NH_2-terminal kinase (JNK) and inhibitory κB kinase (IKK). These pathways play an important role in the development of insulin resistance and diabetes by controlling the inflammatory responses in metabolic tissues, the inhibition of insulin receptor signaling, and the disruption of systemic glucose and lipid homeostasis (4–10). Evidence emerging from experimental models has demonstrated that suppression of these broad inflammatory networks generally results in protection against obesity-induced insulin resistance and diabetes (4–7,11–13). However, the translation of these discoveries to the clinic has been slowed by the lack of effective therapeutic entities, and it remains to be determined whether these strategies may be effective interventions after the establishment of disease.

Department of Genetics and Complex Diseases, Harvard School of Public Health, Boston, MA

Corresponding author: Gökhan S. Hotamisligil, ghotamis@hsph.harvard.edu.

Received 28 June 2013 and accepted 17 October 2013.

T.N. is currently affiliated with the Divisions of Endocrinology and Developmental Biology, Cincinnati Children's Hospital Medical Center, Cincinnati, Ohio.

See accompanying commentary, p. 393.

Given that metaflammation—the chronic, low-grade, metabolic inflammation characteristic of obesity—is critical in the regulation of systemic metabolic homeostasis, there is an emerging emphasis on signaling nodes and molecules that integrate pathogen and stress responses with metabolic pathways as promising targets in understanding and eventually treating these debilitating diseases. In search of such molecules that integrate endoplasmic reticulum (ER) stress and related signaling pathways with inflammatory output, insulin action, and metabolic control, we recently identified the double-stranded RNA–dependent kinase (PKR) (14). PKR is activated by nutrients such as fatty acids and by ER stress, controls major inflammatory cascades such as JNK, and is required for inflammasome activity (14–16). PKR also directly interacts with insulin receptor signaling components and inhibits insulin action (14). There is marked activation of PKR in liver and adipose tissue of mice with dietary and genetic obesity, and two independent lines of PKR-deficient mice have been shown to be protected against obesity-induced insulin resistance and obesity-induced inflammatory changes (14,17). Finally, the ER stress pathways, JNK, and PKR are significantly activated in human obesity, particularly in adipose and liver tissues, raising the possibility that PKR may represent a suitable target for drug development against diabetes (18–20).

Based on these observations, in this study we investigated the potential of pharmacological inhibitors of PKR activity to ameliorate the inflammation and insulin resistance associated with obesity in an established disease model.

RESEARCH DESIGN AND METHODS

Biochemical Reagents

All biochemical reagents were purchased from Sigma-Aldrich (St. Louis, MO) unless otherwise indicated. Anti-insulin receptor substrate (IRS)-1 and anti-phospho-IRS1 (Ser307) were from Upstate Biotechnology (Lake Placid, NY). Antibodies against PKR, JNK1, Akt, phospho-Akt, insulin receptor-β subunit (IRβ), and β-tubulin were from Santa Cruz Biotechnology (Santa Cruz, CA). Anti-phospho-eukaryotic translation initiation factor 2-α (eIF2α; Ser52) antibody was purchased from Invitrogen (Carlsbad, CA). Anti-phospho-insulin receptor (Tyr1162/1163), PKR inhibitor ($C_{13}H_8N_4OS$, imoxin), and a negative control of PKR inhibitor ($C_{15}H_8Cl_3NO_2$) were purchased from Calbiochem (Gibbstown, NJ). Anti-phospho-JNK (Thr183/Tyr185) antibody was purchased from Cell Signaling Technology (Danvers, MA). Recombinant IRS1, JNKs, p38, IKKβ, IκB, myelin basic protein, and agarose-conjugated PKR antibody were purchased from Millipore (Billerica, MA).

Kinase Assays

For in vitro kinase assays, each recombinant protein—at a concentration of 10 ng/μL—was mixed with 16.7 μmol/L PKR inhibitor or DMSO in kinase buffer (25 mmol/L Tris-HCl [pH 7.5], 5 mmol/L β-glycerophosphate, 2 mmol/L dithiothreitol, 0.1 mmol/L Na_3VO_4, 10 mmol/L $MgCl_2$) and was kept on ice for 10 min. Then, the mixture was incubated with a substrate for each measurement and 10 μCi ^{32}P-γATP at 30°C for 20 min followed by SDS-PAGE. For PKR kinase assay with tissue or cell lysates containing 100–300 μg protein, the lysates were mixed with agarose-conjugated PKR antibody or 1 μg PKR antibody and protein G-sepharose beads. The mixture was agitated at 4°C for 3 h, pelleted by centrifugation, and washed three times with lysis buffer followed by two additional washes with PKR kinase buffer (15 mmol/L HEPES [pH 7.4], 10 mmol/L $MgCl_2$, 40 mmol/L KCl, and 2 mmol/L dithiothreitol) for equilibration. After washing with kinase buffer, the beads were incubated in 20 μL kinase buffer containing 10 μCi ^{32}P-γATP (PerkinElmer, Waltham, MA) at 30°C for 20 min followed by SDS-PAGE.

Mice

Animal care and experimental procedures were performed with approval from animal care committees of Harvard University. Age-matched lean and obese *ob/ob* male mice, purchased from The Jackson Laboratory (Bar Harbor, ME) were treated by daily subcutaneous injection with 0.5 mg/kg (200–250 μL) imoxin or vehicle (DMSO/PBS ratio 1:19) for 4 weeks beginning at 9 weeks of age. After 9 days of treatment, an intraperitoneal glucose tolerance test (GTT) was performed (0.5 g/kg glucose) after an overnight food withdrawal. After 16 days of treatment, an intraperitoneal insulin tolerance test (ITT) (2 IU/kg insulin) was performed after 6 h of daytime food withdrawal. Vehicle (0.5% carboxymethylcellulose) or 2-aminopurine (2-AP) (100 mg/kg/day, 100–150 μL) was administered daily to male *ob/ob* mice by oral gavage for 3 weeks beginning at 7 weeks of age. After 1 week of treatment, intraperitoneal GTTs were performed as described above. Intraperitoneal ITTs were performed after 2 weeks of 2-AP treatment.

Hyperinsulinemic–Euglycemic Clamp Studies

Hyperinsulinemic–euglycemic clamps were performed in *ob/ob* mice after 18 days of PKR inhibitor treatment as described previously (14) with slight modification. Four days before the clamp experiments, the right jugular vein of each mouse was catheterized with a polyethylene tube filled with heparin solution (100 units/mL). After an overnight food withdrawal, high-performance liquid chromatography–purified ^{3}H-glucose (0.05 μCi/min; PerkinElmer) was infused during the 2-h basal period. After the basal period, a 120-min hyperinsulinemic–euglycemic clamp was conducted with a primed-continuous infusion of human insulin (Novolin; Novo Nordisk) at a rate of 12.5 mU/kg/min. Blood samples were collected at 20-min intervals for the immediate measurement of plasma glucose concentration, and 25% glucose was

infused at variable rates to maintain plasma glucose at basal concentrations. Insulin-stimulated whole-body glucose disposal was estimated with a continuous infusion of ^{3}H-glucose throughout the clamps (0.1 μCi/min). To estimate insulin-stimulated glucose uptake in individual tissues, 2-^{14}C-deoxyglucose (PerkinElmer) was administered as a bolus (10 μCi) 75 min after the start of clamps. Blood samples were collected for the determination of plasma ^{3}H-glucose, $^{3}H_2O$, and 2-^{14}C-deoxyglucose concentrations. After euthanasia, gastrocnemius muscles from both hindlimbs and epididymal adipose tissue were harvested and immediately frozen in liquid N_2 and stored at −80°C until further analysis. For metabolic cage studies, mice were placed in an indirect open-circuit calorimeter (Columbus Instruments). Mice were afforded access to food and water, and data collections were made over 24 h after a 24-h acclimation period.

Portal Vein Insulin Infusion and Protein Extraction From Tissues

After food withdrawal, mice were anesthetized with an intraperitoneal injection of tribromoethanol (250 mg/kg), and insulin (2 IU/kg) or PBS was injected into mice through the portal vein. Three minutes after injection, tissues were removed, frozen in liquid nitrogen, and kept at −80°C until processing. For protein extraction, tissues were placed in a cold lysis buffer (25 mmol/L Tris-HCl [pH 7.4], 1 mmol/L EGTA, 1 mmol/L EDTA, 10 mmol/L $Na_4P_2O_7$, 10 mmol/L NaF, 2 mmol/L Na_3VO_4, 1% NP-40, 1 mmol/L PMSF, and 1% protease inhibitor cocktail). After homogenization on ice, the tissue lysates were centrifuged, and the supernatants were used for Western blot analysis.

RESULTS

Imoxin Inhibits PKR Action In Vitro and In Vivo

We previously showed that activated PKR inhibits insulin signaling, at least in part, through the induction of IRS1 serine phosphorylation, in vitro and in vivo. This finding prompted our efforts to determine whether a chemical inhibitor of PKR activation could ameliorate insulin resistance, which is considered one of the principal drivers of metabolic syndrome. To this end, we selected an imidazolo-oxindole PKR inhibitor (imoxin), which was previously reported to inhibit PKR kinase activity and autophosphorylation (21,22). We first examined the ability of PKR to directly phosphorylate IRS1 in the presence or absence of imoxin in vitro. Addition of imoxin inhibited PKR activity and suppressed phosphorylation of IRS1 (Fig. 1*A*) and eIF2α (Fig. 1*B*). PKR-induced phosphorylation of IRS1 and eIF2α was not altered by a derivative of inactive oxindole, which served as a negative control (Fig. 1*A* and *B*).

To confirm imoxin action in cells, we treated mouse embryonic fibroblasts (MEFs) with tumor necrosis factor-α (TNF-α), which induces both PKR activation and IRS1 serine phosphorylation. In this system, imoxin treatment effectively reduced TNF-α-induced IRS1 serine phosphorylation (Fig. 1*C*). Imoxin treatment also blocked activation of PKR in response to thapsigargin-induced ER stress (Fig. 1*D*). We previously showed that PKR acts as an upstream regulator of JNK in response to metabolic or organelle stress, and that genetic disruption of PKR activity uncouples these signals from JNK activation and downstream events. Accordingly, we observed here that chemical inhibition of PKR suppressed JNK activation in cells (Fig. 1*E*). Because imoxin does not directly modify JNK activity in vitro (Fig. 1*F*), we conclude that the inhibition of JNK activation occurs downstream of PKR inactivation in cells. As additional controls, we examined whether activity of the closely related kinase PKR-like ER kinase (PERK) and several other functionally relevant enzymes was altered in the presence of imoxin. Although imoxin treatment dose-dependently decreased PKR function and levels of phospho-JNK, these experiments did not reveal any effect of imoxin against PERK (Fig. 1*D*), which is further evidence of selectivity of the inhibitor at least against these structurally or functionally related molecules. We also did not find any direct inhibitory activity of imoxin against any one of the JNK isoforms (Fig. 1*F*), p38 (Fig. 1*G*), or IKKβ (Fig. 1*H*) in in vitro kinase assays.

To determine the efficacy of imoxin treatment in PKR inhibition in vivo, we treated genetically obese (*ob/ob*) mice with the inhibitor for 30 days (0.5 mg/kg/day s.c.). Imoxin treatment markedly reduced PKR levels and PKR activity in white adipose tissue (WAT) (Fig. 1*E*). PKR expression is induced upon PKR activation; thus, the reduction in total PKR level may be a reflection of decreased inflammation in imoxin-treated mice, and is further support that this chemical targeted PKR and reduced its activity. Indeed, in accordance with our findings in cell lines, PKR inhibition also resulted in reduced JNK activity in the WAT of these mice.

Metabolic Outcomes Upon Inhibition of PKR Activity in Obese and Diabetic Mice

To assess the effect of PKR inhibition on glucose homeostasis, we examined body weight and glucose homeostasis in wild-type and *ob/ob* mice after daily subcutaneous administration of imoxin or vehicle for 4 weeks. Imoxin had no effect on body weight in either genotype over the course of the experiment (data not shown), but markedly improved glucose tolerance in *ob/ob* mice compared with the vehicle treatment (Fig. 2*A*). Imoxin-treated *ob/ob* mice also demonstrated significantly improved insulin sensitivity in an ITT (Fig. 2*B*). Treatment with imoxin did not produce adverse effects in liver or kidney function, as determined by alanine aminotransferase (ALT)/aspartate aminotransferase (AST) ratio and blood urea nitrogen level, respectively (Fig. 2*C*). PKR inhibition also did not alter glucose tolerance or insulin tolerance in lean control mice (Fig. 2*D* and data not shown).

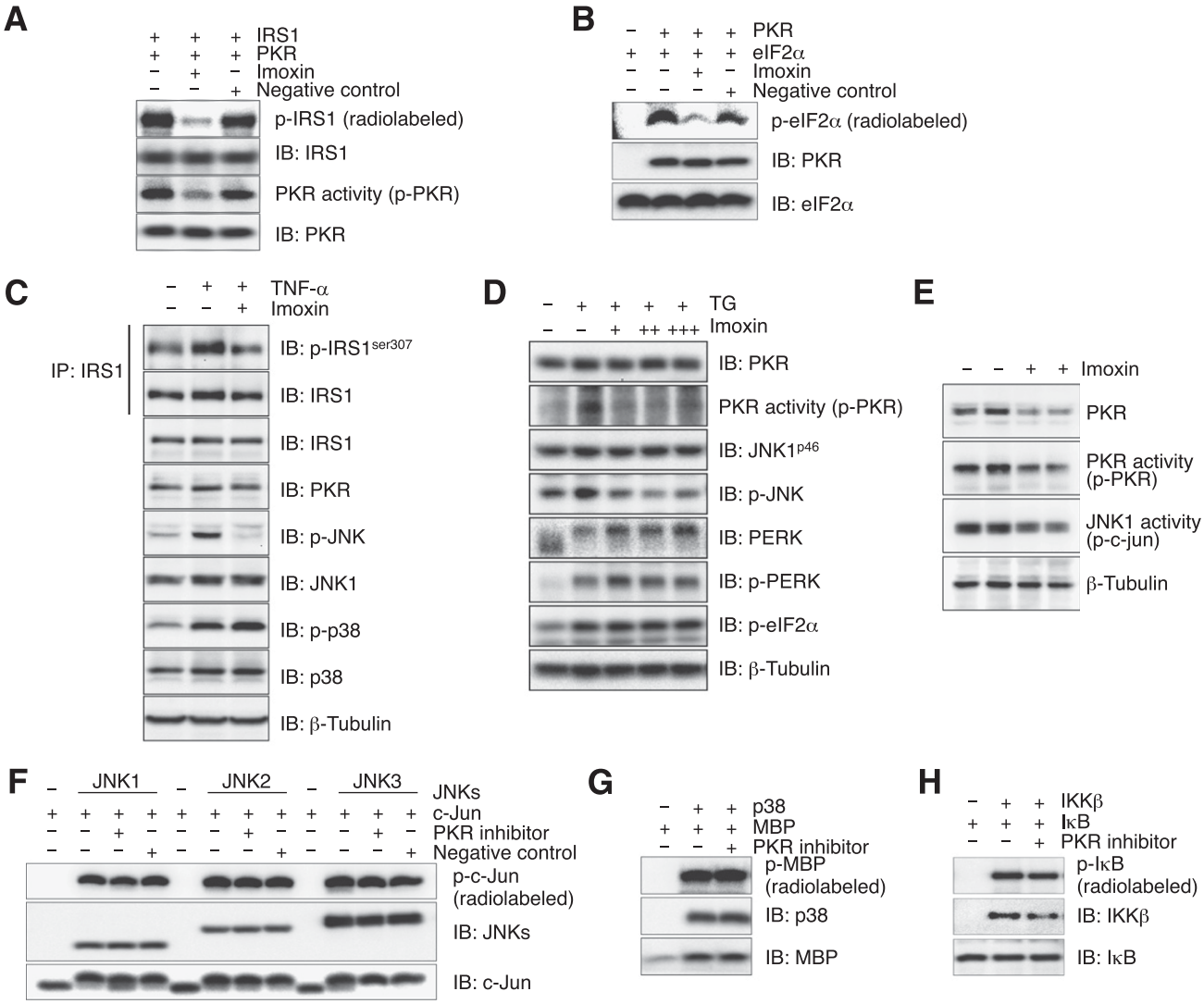

Figure 1— Imoxin inhibits PKR activity in vitro and in vivo. PKR activity was assessed by in vitro kinase assay of PKR with IRS1 (*A*) or eIF2α (*B*) as substrates in the presence or absence of 16.7 μmol/L imoxin as indicated. An oxindole compound was used as a negative control for PKR inhibitor. PKR, IRS1, and eIF2α protein levels were examined by immunoblotting. *C*: TNF-α–induced IRS1 phosphorylation in wild-type MEFs. Cells were pretreated with 1 μmol/L imoxin before the addition of 10 ng/mL TNF-α for 3 h. IRS1 immunoprecipitates and cell lysates were analyzed by Western blot. *D*: Effect of PKR inhibitor (imoxin) on ER stress–induced PERK phosphorylation in wild-type MEFs. Cells were pretreated with imoxin (0.2, 0.5, or 1 μmol/L) before adding 300 nmol/L thapsigargin (TG) for 3 h. Cell lysates were analyzed by Western blot. PKR activity was assessed by the autophosphorylation level of PKR using $ATP^{[g\text{-}32P]}$. *E*: PKR activity and expression and JNK1 activity in WAT of *ob/ob* mice after 30 days of treatment with vehicle or PKR inhibitor (imoxin). PKR and JNK activities were examined by kinase assay. *In vitro* assay of JNK1, JNK2, and JNK3 (*F*); p38 (*G*); and IKKβ (*H*) kinase activity with substrates in the presence or absence of PKR inhibitor are as indicated. p, phospho; IB, immunoblot; IP, immunoprecipitate; MBP, myelin basic protein; IκB, inhibitor of the nuclear factor κB.

Histological examination of the tissue samples revealed that imoxin treatment did not markedly alter adipocyte size in *ob/ob* mice. However, the appearance of crown-like structures, indicative of mononuclear cellular infiltration, was reduced in imoxin-treated animals compared with the vehicle-treated controls (Fig. 2*E*). Expression of the inflammatory markers *Tnfa* and *Il6* in WAT was also significantly reduced in *ob/ob* mice treated with imoxin compared with controls (Fig. 2*F*). We next examined whether inhibition of PKR, the alterations seen in inflammatory mediators, and the reduced JNK activity in WAT culminated in enhanced insulin action. Indeed, insulin-stimulated tyrosine phosphorylation of IRβ and serine phosphorylation of AKT were significantly increased in WAT of imoxin-treated *ob/ob* mice compared with that of vehicle-treated controls (Fig. 2*G*). Thus, systemic PKR inhibition by a small molecule reduces adipose tissue inflammation and increases insulin sensitivity in WAT of *ob/ob* mice.

To further explore the therapeutic potential of PKR inhibition and generate more confidence in the chemical PKR inhibition approach, we also tested a second small

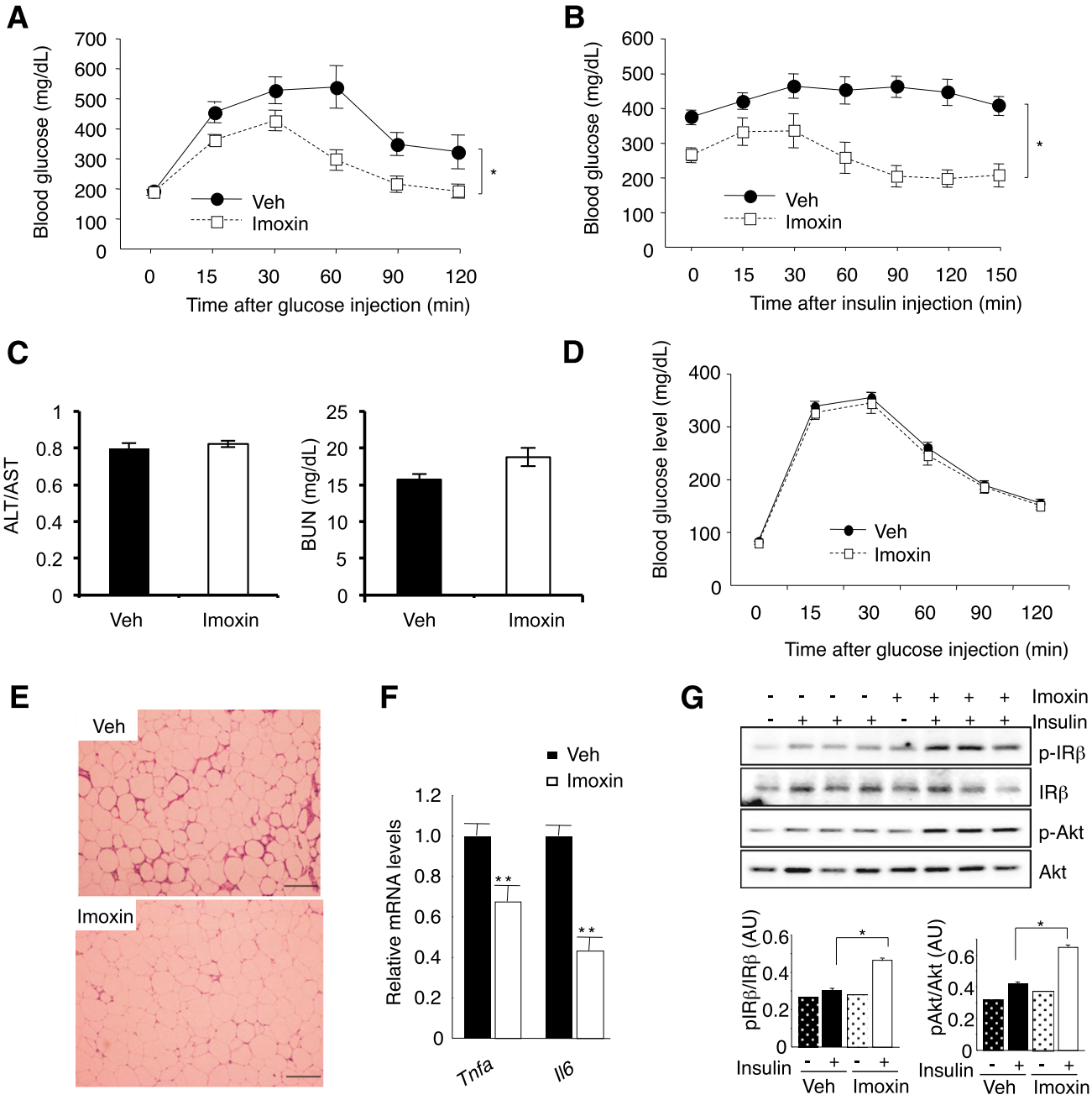

Figure 2—Imoxin improves glucose homeostasis and reduces inflammation in genetically obese mice. *A*: GTTs performed after 9 days of treatment in *ob/ob* mice with vehicle (Veh) (n = 6) or imoxin (n = 6). *B*: ITTs performed after 16 days of treatment in *ob/ob* mice with vehicle (n = 6) or imoxin (n = 6). *C*: ALT/AST ratio and blood urea nitrogen (BUN) levels were measured in the serum of *ob/ob* mice treated with vehicle (n = 7) or imoxin (n = 8). *D*: GTT was performed on male C57BL/6J mice after 24 days of treatment with vehicle or imoxin. *E*: Hematoxylin-eosin staining of WAT from *ob/ob* mice treated with vehicle or imoxin for 35 days. Scale bar, 200 μm. *F*: Expression of *Tnfa* and *Il6* in WAT of *ob/ob* mice treated with vehicle (n = 5) or imoxin (n = 5). *G*: Insulin-stimulated IRβ tyrosine 1162/1163 and Akt serine 473 phosphorylation in WAT of *ob/ob* mice treated with vehicle or imoxin. Quantification of the Western blot band intensity is shown in the lower panels. Data are shown as the mean ± SEM. *P < 0.05; **P < 0.01. The statistical difference between groups was calculated by two-way ANOVA. p, phospho.

molecule, 2-AP, an established inhibitor of PKR that is structurally independent of imoxin (23). In *ob/ob* mice, oral administration of 2-AP (200 mg/kg/day) improved glucose tolerance and insulin-stimulated glucose disposal (Fig. 3*A* and *B*). In adipose tissue from 2-AP–treated mice, we also observed a reduction in the expression of proinflammatory cytokines and macrophage markers (Fig. 3*C*). Furthermore, we found that serum levels of both ALT and AST were reduced by treatment with 2-AP, suggesting that 2-AP treatment potentially also improves liver function (Fig. 3*D* and *E*). Together, these results support the concept that PKR inhibition may

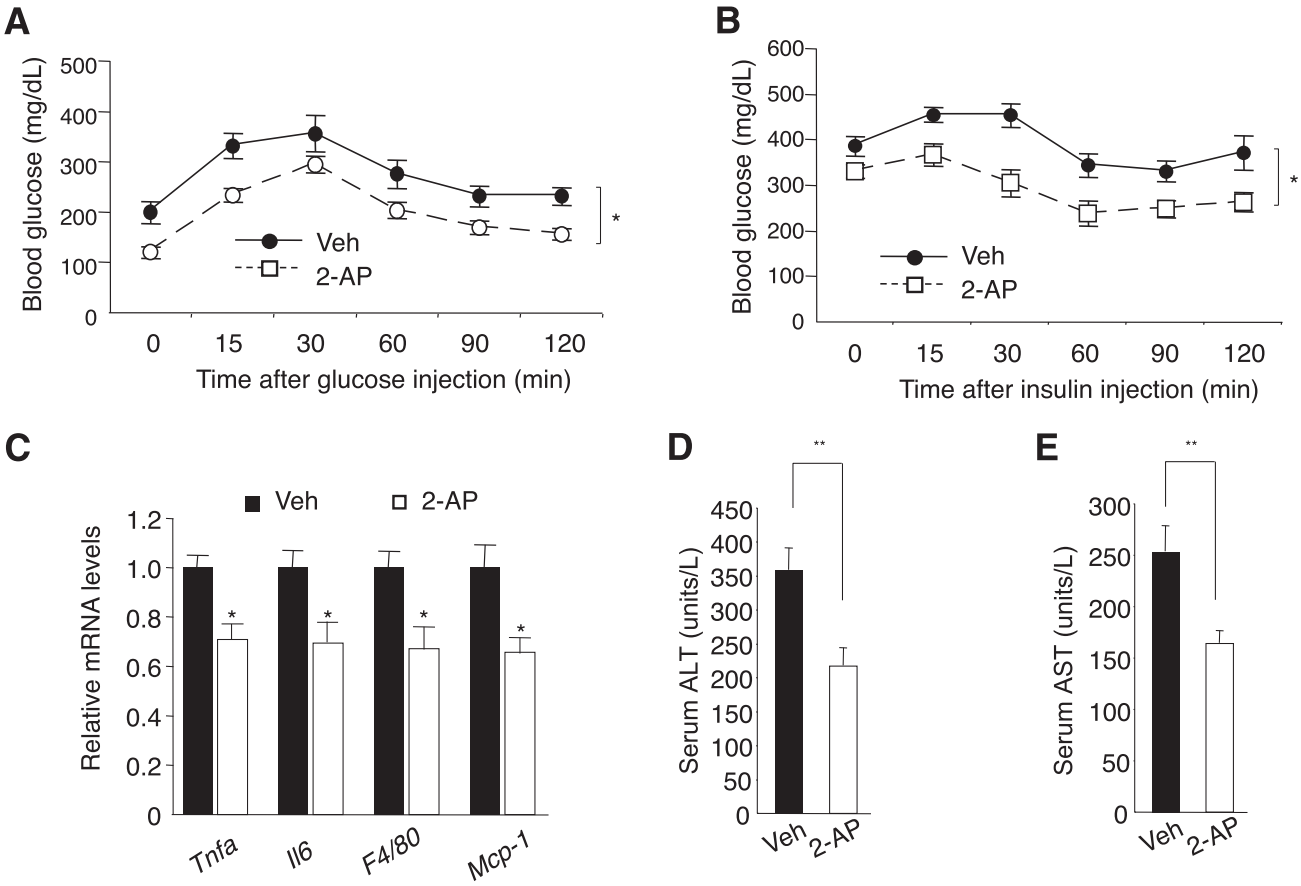

Figure 3—The PKR inhibitor 2-AP improves glucose homeostasis in *ob/ob* mice. *A*: GTTs performed after 7 days of treatment in *ob/ob* mice with vehicle (Veh) ($n = 8$) or 2-AP ($n = 8$). *B*: ITTs performed after 14 days of treatment in *ob/ob* mice with vehicle ($n = 8$) or 2-AP ($n = 8$). *C*: Expression of *Tnfa*, *Il6*, *F4/80*, and *Mcp-1* in WAT of *ob/ob* mice treated with vehicle ($n = 8$) or 2-AP ($n = 8$) for 21 days. *D* and *E*: Serum ALT and AST levels in *ob/ob* mice after 21 days of treatment with vehicle ($n = 9$) or 2-AP ($n = 9$). Data are shown as the mean ± SEM. $^*P < 0.05$; $^{**}P < 0.01$. The statistical difference between groups was calculated by two-way ANOVA.

generate metabolic benefits in mice with established disease.

Effect of PKR Inhibition on Whole-Body Energy Metabolism, Glucose Fluxes, and Insulin Sensitivity

We previously observed that $PKR^{-/-}$ mice displayed higher rates of oxygen consumption than control mice, likely contributing to their decreased weight (14). This raised the possibility that the metabolic benefits of PKR deletion may be secondary to reduced weight, although PKR-deficient animals were also protected against a short-term model of insulin resistance (14). To determine whether small-molecule inhibition of PKR similarly altered the metabolic phenotype, we performed metabolic cage studies on *ob/ob* mice treated with vehicle or imoxin. PKR inhibition did not alter V_{O_2} (Fig. 4*A*) or heat production (Fig. 4*B*), indicating that PKR-mediated regulation of glucose homeostasis is not dependent on weight regulation mechanisms.

To better understand the whole-body consequences of PKR inhibition on insulin sensitivity and glucose fluxes, we next performed hyperinsulinemic–euglycemic clamp studies in *ob/ob* mice after 18 days of treatment with imoxin. The glucose infusion rate required to maintain blood glucose levels was significantly higher in imoxin-treated mice compared with vehicle-treated controls (Fig. 4*C* and *D*), indicating increased systemic insulin sensitivity. Insulin-stimulated glucose disposal rate and suppression of hepatic glucose production (HGP) were significantly enhanced by imoxin treatment (Fig. 4*E* and *F*). There was no significant difference in basal HGP between the vehicle and imoxin groups (Fig. 4*G*). Imoxin treatment also induced a small but significant increase in insulin-stimulated glucose uptake in muscle (Fig. 4*H*). These data demonstrate that chemical inhibition of PKR improves whole-body insulin sensitivity through the suppression of insulin-stimulated HGP and the enhancement of glucose disposal in peripheral tissues.

DISCUSSION

Understanding the molecular links between obesity and metabolic syndrome may suggest novel therapeutic strategies and targets for the treatment of this prevalent

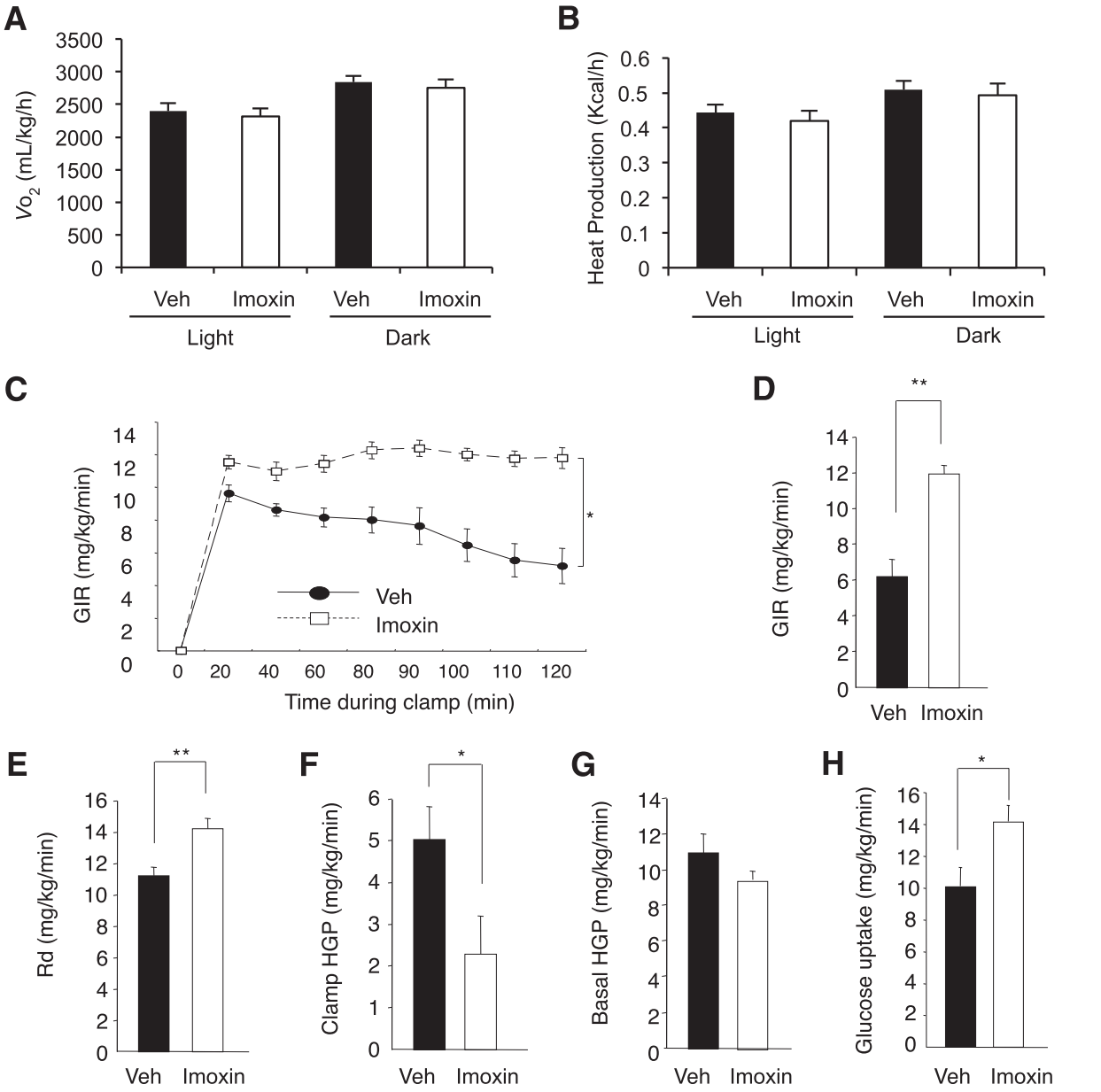

Figure 4—Imoxin treatment improves systemic insulin sensitivity without altering metabolic rate. Metabolic cage studies were performed on *ob/ob* mice treated with vehicle (Veh) (n = 10) or imoxin (n = 10). *A*: Rate of Vo_2. *B*: Heat production. Hyperinsulinemic–euglycemic clamp studies were performed in *ob/ob* mice after 18 days of treatment with vehicle (n = 8) or imoxin (n = 5). *C*: Glucose infusion rates (GIRs) during the clamp procedure. *D*: Average (GIR). *E*: Whole-body glucose disposal rates (Rd). *F*: HGP during the clamp. *G*: Basal HGP. *H*: Tissue glucose uptake in gastrocnemius muscle. Data are shown as the mean ± SEM. $^*P < 0.05$; $^{**}P < 0.01$.

disease. Our group and others have previously found that PKR is activated in adipose and other tissues during obesity in mouse models and in obese humans, and is critical to the development of metaflammation and insulin resistance. Studies in two independent lines of PKR deficiency in mice showed protection against insulin resistance and diabetes (14,17). Hence, we examined whether pharmacological inhibition of PKR action could reduce obesity-induced insulin resistance and metabolic dysfunction. Here, we find that two distinct small-molecule chemical inhibitors of PKR kinase activity improved glucose homeostasis and insulin sensitivity, and ameliorated adipose inflammation in genetically obese mice. Thus, our findings suggest that PKR inhibition may be a viable interventional strategy in the treatment of established metabolic disorders.

In this study, PKR inhibition had no effect on glucose tolerance or insulin sensitivity in lean mice, in agreement with our previous finding of normal glucose homeostasis in lean PKR knock-out animals (14). This suggests that, despite its role as a nutrient and stress sensor, PKR activity is dispensable for the modulation of insulin

responsiveness and adipose inflammation under homeostatic conditions. An independent study has suggested that PKR deficiency resulting from a deletion in the RNA-binding domain may increase insulin sensitivity and metabolic health even in lean animals (17). Hence, it is possible that the inhibition achieved through synthetic chemical inhibition is not fully replicating these observations in the lean mice with whole-body genetic ablation of PKR or that there are subtle differences in the deletion models. Nevertheless, human studies (18–20) and multiple genetic models (14,17) have provided evidence supporting the consideration of this enzyme for therapeutic purposes and should stimulate the development of orally active molecules with enhanced pharmacological properties. Total-body PKR deficiency in mice does not appear to be associated with major immunological complications. However, it is worth noting that, in addition to cellular stress signals, PKR can sense pathogens and plays an important role in inflammasome activation (16). Hence, it will be important to examine whether systemic PKR inhibition as used in this paradigm would hinder inflammatory responses to infection, especially under long-term usage, and to consider alternative targeting strategies.

Our findings here also suggest that blocking PKR activity in established disease models has the ability to provide benefits independent of body weight regulation. This raises some interesting possibilities for testing the efficacy of PKR blockade in other diseases. For example, PKR has previously been implicated in mediating β-cell death as part of the antiviral response that may precipitate the development of type 1 diabetes in some patients (23). Thus, in addition to our finding that PKR inhibitors can improve glucose homeostasis in a mouse model of insulin resistance and type 2 diabetes, PKR inhibitors may also have potential as early interventional agents in type 1 diabetes models or other chronic metabolic diseases associated with similar stress, inflammatory, and/or metabolic underpinnings.

In conclusion, this work further supports the hypothesis that PKR plays an important role in integrating nutrient and stress signaling, and the progression and persistence of insulin resistance during obesity. As the global chronic metabolic disease epidemic continues, it will be critical to identify new therapeutic entities that can be used to both prevent metabolic disease from developing and to treat individuals after pathologies such as insulin resistance occur. These findings suggest PKR inhibitors may offer a strategy to alleviate metaflammation and serve as potential agents to fill this niche.

Acknowledgments. The authors thank Kathryn Claiborn, Harvard School of Public Health, for editorial input.

Funding. T.N. was supported by a fellowship from the Human Frontier Science Program and is currently supported by a grant from the American Heart Association. This work is supported in part by a grant from the National Institutes of Health to G.S.H. (DK052539).

Duality of Interest. No potential conflicts of interest relevant to this article were reported.

Author Contributions. T.N. conceived the hypothesis, designed and performed experiments, analyzed the results, and wrote the manuscript. A.A., B.B., and M.F. performed experiments and analyzed results. G.S.H. conceived the hypothesis, designed the experiments, analyzed the results, and wrote the manuscript. G.S.H. is the guarantor of this work and, as such, had full access to all the data in the study and takes responsibility for the integrity of the data and the accuracy of the data analysis.

References

1. Hotamisligil GS. Inflammation and metabolic disorders. Nature 2006;444:860–867
2. Hotamisligil GS, Erbay E. Nutrient sensing and inflammation in metabolic diseases. Nat Rev Immunol 2008;8:923–934
3. Baker RG, Hayden MS, Ghosh SNF. NF-κB, inflammation, and metabolic disease. Cell Metab 2011;13:11–22
4. Arkan MC, Hevener AL, Greten FR, et al. IKK-beta links inflammation to obesity-induced insulin resistance. Nat Med 2005;11:191–198
5. Cai D, Yuan M, Frantz DF, et al. Local and systemic insulin resistance resulting from hepatic activation of IKK-beta and NF-kappaB. Nat Med 2005;11:183–190
6. Hirosumi J, Tuncman G, Chang L, et al. A central role for JNK in obesity and insulin resistance. Nature 2002;420:333–336
7. Kaneto H, Nakatani Y, Miyatsuka T, et al. Possible novel therapy for diabetes with cell-permeable JNK-inhibitory peptide. Nat Med 2004;10:1128–1132
8. Osborn O, Olefsky JM. The cellular and signaling networks linking the immune system and metabolism in disease. Nat Med 2012;18:363–374
9. Chawla A, Nguyen KD, Goh YPS. Macrophage-mediated inflammation in metabolic disease. Nat Rev Immunol 2011;11:738–749
10. Shoelson SE, Lee J, Goldfine AB. Inflammation and insulin resistance. J Clin Invest 2006;116:1793–1801
11. Nakatani Y, Kaneto H, Kawamori D, et al. Modulation of the JNK pathway in liver affects insulin resistance status. J Biol Chem 2004;279:45803–45809
12. Wunderlich FT, Luedde T, Singer S, et al. Hepatic NF-kappa B essential modulator deficiency prevents obesity-induced insulin resistance but synergizes with high-fat feeding in tumorigenesis. Proc Natl Acad Sci USA 2008;105:1297–1302
13. Reilly SM, Chiang SH, Decker SJ, et al. An inhibitor of the protein kinases TBK1 and IKK-ε improves obesity-related metabolic dysfunctions in mice. Nat Med 2013;19:313–321
14. Nakamura T, Furuhashi M, Li P, et al. Double-stranded RNA-dependent protein kinase links pathogen sensing with stress and metabolic homeostasis. Cell 2010;140:338–348
15. Komiya K, Uchida T, Ueno T, et al. Free fatty acids stimulate autophagy in pancreatic β-cells via JNK pathway. Biochem Biophys Res Commun 2010;401:561–567
16. Lu B, Nakamura T, Inouye K, et al. Novel role of PKR in inflammasome activation and HMGB1 release. Nature 2012;488:670–674
17. Carvalho-Filho MA, Carvalho BM, Oliveira AG, et al. Double-stranded RNA-activated protein kinase is a key modulator of insulin sensitivity in physiological conditions and in obesity in mice. Endocrinology 2012;153:5261–5274
18. Boden G, Duan X, Homko C, et al. Increase in endoplasmic reticulum stress-related proteins and genes in adipose tissue of obese, insulin-resistant individuals. Diabetes 2008;57:2438–2444

19. Gregor MF, Yang L, Fabbrini E, et al. Endoplasmic reticulum stress is reduced in tissues of obese subjects after weight loss. Diabetes 2009;58:693–700
20. Carvalho BM, Oliveira AG, Ueno M, et al. Modulation of double-stranded RNA-activated protein kinase in insulin sensitive tissues of obese patients. Obesity 2013;21:2452–2457
21. Eley HL, Russell ST, Tisdale MJ. Attenuation of muscle atrophy in a murine model of cachexia by inhibition of the dsRNA-dependent protein kinase. Br J Cancer 2007;96:1216–1222
22. Jammi NV, Whitby LR, Beal PA. Small molecule inhibitors of the RNA-dependent protein kinase. Biochem Biophys Res Commun 2003;308:50–57
23. Hu Y, Conway TW. 2-Aminopurine inhibits the double-stranded RNA-dependent protein kinase both in vitro and in vivo. J Interferon Res 1993;13:323–328
24. Scarim AL, Arnush M, Blair LA, et al. Mechanisms of β-cell death in response to double-stranded (ds) RNA and interferon-γ: dsRNA-dependent protein kinase apoptosis and nitric oxide-dependent necrosis. Am J Pathol 2001;159:273–283